Journal of Radiation and Nuclear Applications
An International Journal

http://dx.doi.org/10.18576/jrna/110207

Investigation of Gamma Radiation Shielding Capability of Fabricated Concrete Doped Coconut Shell Ash Using WinXcom

I. Abdul Malik, I. Ibrahim, M. M. Idris, M. A. Sidi, A. S. Nuhu and M. S. Ogande.*

Nasarawa State University, Keffi, Nigeria.

Received: 25 Dec. 2025, Revised: 15 Feb. 2026, Accepted: 1 Mar. 2026
Published online: 1 May. 2026

Abstract: The usage of radioactive sources has grown recently due to the advancement of nuclear science and technology in a variety of disciplines, including nuclear research facilities, nuclear power plants, space exploration, and medical care. This study is aimed at investigating the gamma radiation shielding capability of fabricated concrete doped with coconut shell ash at different mixing ratios (x=5, 10, 15, 20, 25, 30, 35, 40) wt%, and X-ray Fluorescence (XRF) technique was used to determine the elemental composition of the composites, WinXcom software were used to generate the attenuation coefficients. The result shows that the maximum (minimum) mass attenuation coefficient values were obtained at photon energies of 0.02 (15.00) MeV for all samples (A1-A8), which shows a reduction in MAC values as energy increases for the entire sample. The trend of the linear attenuation coefficient appears to be similar to that of the mass attenuation coefficient. The half-value thickness and mean free path appear to be similar and generally increase with photon energy for all the samples. These indicate that penetration is directly proportional to the energy of photons; hence, for higher energy photons, a thicker absorbing material is required. The fabricated concrete doped with coconut shell ash shows better attenuation capability than ordinary concrete and slightly below the shielding capability of lead.

Keywords: Linear Attenuation Coefficient, Mass Attenuation Coefficient, Half Value Layer.

1 Introduction

Microsoft Word Gamma radiations have proven to be the most challenging to control out of all the radiations produced by radioactive materials [1]. This is because gamma radiation has greater penetrating power. Solid-state tailored materials with a relatively high density and good radiation shielding capabilities could be used to effectively shield against gamma radiation [2]. The usage of radioactive sources has grown recently due to the advancement of nuclear science and technology in a variety of disciplines, including nuclear research facilities, nuclear power plants, space exploration, medical care, and agriculture. Biological radiation shields must offer employees enough protection at a fair price to ensure safe working conditions. Numerous details concerning photon penetration and energy deposition in biological shielding and other dosimetric materials can be learned from the mass attenuation coefficient [3-6].

The traditional gamma-ray shielding materials are lead and concrete. The rapidly growing nuclear industry and the wide-ranging use of radioactive materials need the search for novel, low-cost shielding alternatives that are locally accessible. The new substance should be reasonably priced, environmentally friendly, and ideally use industrial leftovers. Waste production has multiplied as a result of industrialization. Coal fly ash is one of these wastes, and because of its pozzolanic character, it can be employed in the construction of bricks [7]. Since ancient times, clay has been used to make bricks because it is a naturally occurring material made up of fine-grained minerals that is plastic when wet and hard when dried or fired. Clay soils also have better photon energy absorption properties than other soils [7].

2 Experimental Section

2.1 Materials

The materials that were used are:

Coconut shell husk ash, cement, aggregates (stone and gravel),

*Corresponding author e-mail: sidimuhammad@nsuk.edu.ng

2.2 Theory

2.2.1 Linear Attenuation Coefficient

The linear attenuation coefficient (μ), which is a crucial factor in determining how gamma radiation interacts with incident materials, was explained by [8] as shown in the equation below:

$$\mu = \frac{1}{x} \ln\left(\frac{I}{I_o}\right) \quad (1)$$

Where I_0 is the intensity of the incident gamma-ray photon, while I is the transmitted gamma-ray photons through a target of absorber thickness x.

2.2.2 Mass Attenuation Coefficient

[9] have highlighted that the mass attenuation coefficient (μ/ρ) was calculated to check the ability of the studied materials as shielding to rays without depending on the density of the material, by dividing the experimentally calculated (μ) for a given material by its density (ρ) using the equation below:

$$MAC = \frac{\mu}{\rho} \quad (2)$$

2.2.3 Half-Value Layer (HVL)

This factor is the absorption thickness required to decrease the incident radiation to 50% of its initial value and is evaluated using equation [10]:

$$HVL = \frac{\ln 2}{\mu} \quad (3)$$

2.2.4 Tenth-Value Layer (TVL)

In contrast to the HVL, the TVL measures the thickness needed to reduce gamma radiation intensity to 10% of its initial value. The TVL equation is given as follows [11-12]:

$$TVL = \frac{\ln 10}{\mu} \quad (4)$$

2.2.5 Mean Free Path

The mean free path, mfp, which is defined as the average distance between two successive photon interactions, can be calculated using the equation below [13-14]:

$$MFP = \frac{1}{\mu} \quad (5)$$

2.2.6 Bulk Density

The calculation of the bulk densities of the samples was carried out by measuring the mass of the samples and their respective volumes. According to [15], the formula for calculating the bulk density (ρ_{Bulk}) of the composite is presented below.

$$\rho = \frac{M_{Cement}}{V_{cement}} + \frac{M_{sharp-sand}}{V_{sharp-sand}} + \frac{M_{granite}}{V_{granite}} + \frac{M_{coconut-shell-ash}}{V_{coconut-shell-ash}} \quad (6)$$

Where V is the composite volume, cm^3, M is the mass of the composite component, and ρ is the density of the composite component, g/cm^3.

2.3 Methods

2.3.1 Fabrication and Processing of Concrete – Coconut Shell Ash (CSA) Waste

The coconut shells were picked from piles at some locations in Keffi, Nasarawa State. The shells were washed and dried. The shells were burnt into ashes at a temperature of 200^{0} °C using a muffle furnace. The resulting substances were spread to cool down. After the cooling, the substances were pulverized and sieved with a 2 mm mesh into powdered substances.

2.3.2 Fabrication of Concrete – Coconut Shell Ash (CSA) Composite

The concrete matrix(Aggregates) was mixed with coconut shell ash powder at different percentages by weight, as shown in Table 3.2, to obtain samples A1, A2, A3, A4, A5, A6, A7, and A8 (x = 5, 10, 15, 20, 25, 30, 35, 40)wt%. About 25 ml of water was added to each mixture, stirred, molded into a disc of diameter 20 mm and height 20 mm, and allowed to dry at room temperature for a few days until a constant weight is achieved. The concretes was mixed with 5%, 10%, 15%, 20%, 25%, 30% and 35% of the coconut shell ash at a mixing proportion by weight of 0.475kg: 1kg: 1kg: 0.025kg, 0.45kg: 1kg: 1kg: 0.05kg, 0.425kg: 1kg: 1kg: 0.075kg, 0.4kg: 1kg: 1kg: 0.1kg, 0.375kg: 1kg: 1kg: 0.125kg, 0.35kg: 1kg: 1kg: 0.15kg and 0.325kg: 1kg: 1kg: 0.175kg respectively of cement:sharp-sand:granite: coconut-shell-ash.

Eight (8) samples were made from the mixtures, which are 2 cm thick, labelled sample A1 (5%), A2 (10%), A3 (15%), A4 (20%), A5 (25%), A6 (30%), A7 (35%), and A8 (40%) respectively. The samples were further oven dried at a

lower temperature of about 100 °C for two hours to remove any traces of water content left in the samples.

Table 1: Mixing Proportion of Concrete and Coconut Shell Ash.

Sample code	Concrete Metrix Content% by weight	CSA Content% by weight
A1	95	5
A2	90	10
A3	85	15
A4	80	20
A5	75	25
A6	70	30
A7	65	35
A8	60	40

2.3.3 Elemental Analysis of the Fabricated Composites

The chemical compositions of fabricated concretes were obtained using Thermo Scientific X-ray Fluorescence (XRF) with Model Number ARL-QUANT'X-EDXRF-Analyzer and Serial Number 9952120 (see Figure 1). XRF analysis was done using the standard method with Montana soil SRM 2710 for the Geological Sample, while IAEA – 155 Why Powder for Biological Sample as a Thermo Fisher Scientific standard reference material. Two (2) grams of each of the samples was weighed and then placed on a sample holder and covered with cotton wool to prevent it from spraying.

Fig. 1: ARL QUANT'X EDXRF Analyzer.

Table 2: Elemental Composition of the Samples.

Sample Code	Composition (wt%)									Density (g/cm³)
	Fe_2O_3	SiO_2	Al_2O_3	MgO	P_2O_5	SO_3	CaO	K_2O	SrO	
A1 (5%)	1.075	33.050	8.693	6.923	0.249	1.168	21.490	1.459	4.043	6.238
A2 (10%)	1,251	34.010	7.740	4.958	1.490	1.521	23.46	1.964	4.562	6.422
A3 (15%)	1.188	32.310	7.353	4.710	1.416	1.445	22.290	1.866	4.334	6.476
A4 (20%)	2.158	35.840	1.952	0.897	5.508	2.671	24.610	2.699	4.627	6.501
A5 (25%)	2.050	34.050	1.854	0.852	5.233	2.538	23.380	2.564	4.396	6.638
A6 (30%)	1.359	34.720	4.700	3.845	3.797	1.767	24.170	1.979	4.621	6.722
A7 (35%)	1.291	32.980	4.465	3.653	3.608	1.679	22.960	1.880	4.390	6.876
A8 (40%)	1.226	31.330	4.242	3.470	3.427	1.595	21.820	1.786	4.170	6.976

2.3.5 Evaluation of Radiation Shielding Capability of the Samples

In this study, the gamma radiation shielding capability (GRSC) parameters of the samples were evaluated using WinXCOM software. The quantitative elemental compositions of the samples obtained using EDXRF techniques, as well as their densities, served as input data to the WinXCOM software. The computations are based on Bragg's Law.

In view of validating our subsequent calculations, we first evaluated the linear attenuation coefficient (μ) using WinXCOM software. The obtained values at energies ranging from 0.02 MeV to 15.00 MeV gamma energies using WinXCOM [16-17].

3 Results and Discussion

The WinXCom computer software was used to generate the mass attenuation coefficient for the energy range 0.02 to 15 MeV, presented in Tables. The linear attenuation coefficient, half-value layer, tenth-value, and mean free path values were calculated using Microsoft Excel software and are presented in Figures 1, 2, 3, and 4, respectively.

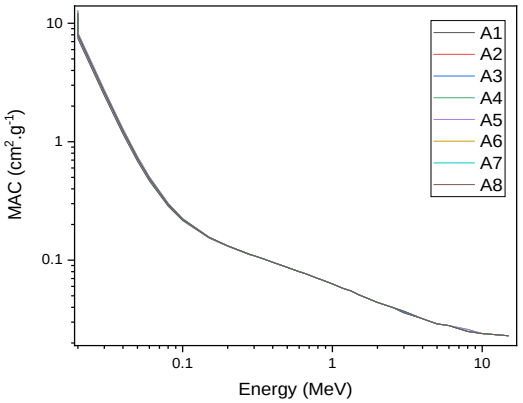

Fig. 2: Mass attenuation coefficient samples.

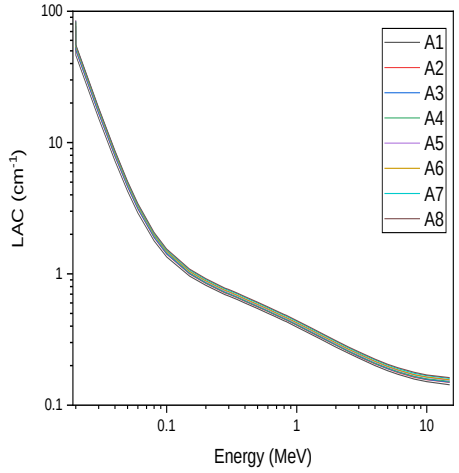

Fig.3: Mass attenuation coefficient samples

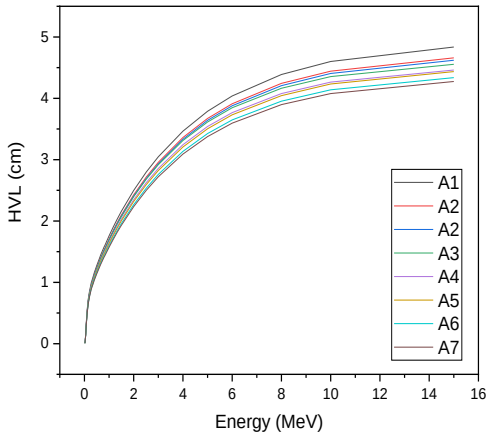

Fig.4: Half Value Layer Spectra of Samples.

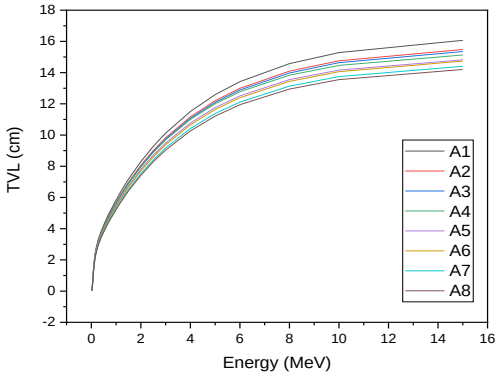

Fig.5: Tenth Value Layer Spectra of Samples.

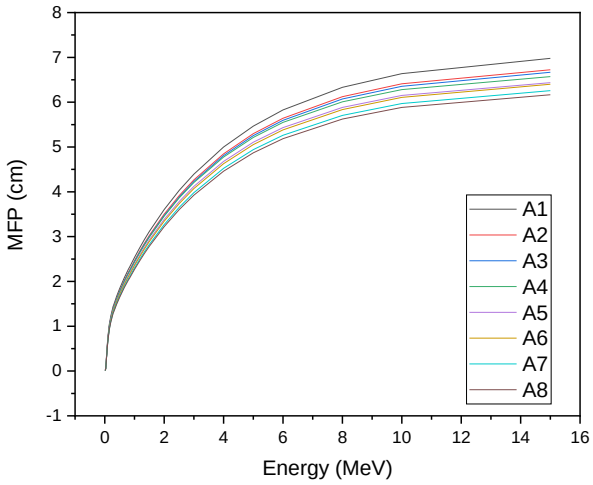

Fig. 6: Mean Free Path of Samples.

The mass attenuation coefficient (MAC) versus photon power spectra of the eight studied fabricated concrete doped with coconut shell ash are presented in Figure 1.

From the figure, the decrease in MAC values from 0.02 to 15 MeV shows a reduction in MAC value as energy increases for the entire sample. Compton scattering is the cause of the observed drop in MAC values as photon energy increases, and at low photon energy, the increase in MAC values is a result of the dominance or prevalence of photoelectric interaction (absorption). For the present fabricated concrete doped coconut shell ash, the maximum (minimum) MAC values were obtained at photon energies of 0.02 (15.00) MeV for all materials (A1-A8).

The variation in the value of the linear attenuation coefficient (LAC) as a function of energy is depicted in Figure 2. It was noted that the mass absorption coefficient and the linear attenuation coefficient seem to follow a similar trend. However, there is a relative difference in the linear attenuation coefficient from that observed for MAC, which is due to the density of the composites. At lower photon energy, LAC values are high, due to dominance of photoelectric absorption, while the reason for the decline in LAC values with increasing photon energy is the increasing significance of Compton scattering.

The half-value layer of photons in the investigated fabricated concrete doped with coconut shell ash as a function of photon energy is presented in Figure 3. The HVL is inverse to that of LAC and MAC. For every sample, the HVL typically increases with photon energy.

As photon energy rises, the contribution of Compton scattering decreases, and photoelectric absorption becomes more significant, increasing HVL values. At lower photon

energy, Compton scattering tends to be the dominant interaction, which leads to a decrease in HVL values. This indicates that higher energy photons appear to be more penetrating; hence, more thickness of absorbing material is required to absorb them.

The tenth value layer of photons in the investigated fabricated concrete doped with coconut shell ash as a function of photon energy is presented in Figure 4. For every sample, the TVL normally improves with photon energy. When photon energy increases, the contribution of Compton scattering decreases and photoelectric absorption becomes more significant, resulting in an increase in TVL values. At lower photon energy, Compton scattering tends to be the dominant interaction, which leads to a decrease in TVL values. This indicates that higher energy photons appear to be more penetrating; hence, more thickness of absorbing material is required to absorb them.

The calculated mean free path as a function of energy is shown in Figure 5. The figure is similar to that of HVL and TVL, and increases with an increase in photon energy due to the contribution of photoelectric absorption interaction being reduced, and Compton scattering dominates the interaction and becomes more significant. This indicates that higher energy photons travel further into the samples due to reduced interaction cross sections of the processes leading to photon absorption. The reduction in the MFP values at lower photon energy is because photoelectric absorption dominates the interaction [18].

4 Conclusions

Fabricated concrete doped with coconut shell ash was investigated in this study using the WinXCom software, which indicates that the maximum (minimum) mass absorption coefficient values were obtained at photon energies of 0.02 (15.00) MeV for all samples (A1-A8), which shows a better shielding capability. The trend of the linear absorption coefficient appears to be similar to that of the mass absorption coefficient. From half-value thickness and tenth-value thickness, it indicates that penetration is directly proportional to the energy of photons; hence, for higher energy photons, a thicker absorbing material is required. The fabricated concrete doped with coconut shell ash shows better attenuation capability than ordinary concrete and slightly below the shielding capability of lead.

Acknowledgement

The authors thankfully acknowledge funding partners for this research.

References

[1]. G. Yilmaz, The effects of temperature on the characteristics of kaolinite and bentonite. *Sci. Res. Essays 6* (9), 1928–1939, 2011.

[2]. H. S. Isfahani, S. M. Abtahi, M. A. Roshanzamir, A. Shirani, & S. M. Hejazi (2018). Permeability and gamma-ray shielding efficiency of clay modified by barite powder, *Geotechnical and Geological Engineering*, *37* (2), 845–855, 2018.

[3] F. Alafer, FH Sallam, M Al Meshari, YAlzamil, A Abanomy, S Alhujaili, A El-Taher., The influence of thermal treatment on the structural properties and gamma rays shielding of bentonite clay ceramic. Radiation Physics and Chemistry 217, 111531. 2024.

[4] A Khalil, Ibrahim I Bondouk, Elhassan A Allam, Islam M Nabil, Mogahed Al-Abyad, Heba Saudi, Atef El-Taher, Mohamed E Mahmoud, Ahmed Amar., 2024 A binary composite material of nano polyaniline intercalated with nano-Fe2O3 for enhancing gamma-radiation-shielding properties: experimental and simulation study. Progress in Nuclear Energy 169, 105067

[5] RM El-Sharkawy., EA Allam., A. El-Taher,., E.R Shaaban. and ME Mahmoud., Synergistic Effect of Nano-bentonite and Nano cadmium Oxide Doping Concentrations on Assembly, Characterization and Enhanced Gamma-Rays Shielding Properties of Polypropylene Ternary Nanocomposites. International Journal of Energy Research. 45 (6), 8942-8959. 2021.

[6] A. El-Taher., H.M Mahmoud and Adel Abbady., 2007 Comparative Study of Attenuation and Scattering of Gamma –Ray through Two Intermediate Rocks. Indian Journal of Pure & Applied Physics, 45.

[7]. N. Kuck, Z. Tumsavas, & M. Cakir, Determining photon energy absorption parameters for different soil samples. *Journal Radiation Research*, *54* (1), 578-586, 2013.

[8] HH Negm, EA Allam, IM Nabil, E Abdeltwab, M Mostafa, A El-Taher., 2024 Exploring the potential of attapulgite clay composites containing intercalated nano-cadmium oxide and nano-nickel oxide for efficient radiation shielding applications. Radiation Physics and Chemistry 225, 112149

[9] U Rilwan, SA Edeh, MM Idris, II Fatima, SF Olukotun, GZ Arinseh, PZ Bonat, A. El-Taher, KA Mahmoud, Taha A Hanafy, MI Sayyed., 2025 Influence of waste glass on the gamma-ray shielding performance of concrete. Annals of Nuclear Energy 210, 110876

[10]. M. A. Kiani, S. J. Ahmadi, M. Outokesh, R. Adeli, & H. Kiani, Study on physico-mechanical and gamma-ray shielding characteristics of new ternary nanocomposites. *Applied Radiation Isotopes*, *143*(1), 141–148, 2019.

[11]. O. Agar, H. O. Tekin, M. I. Sayyed, M. E. Korkmaz, O. Culfa, & C. Ertugay, Experimental investigation of photon attenuation behaviors for concretes including

natural perlite mineral. *Results Physics*, *12*(1), 237–243, 2019.

[12] EA. Allam, , RM. El-Sharkawy., Atef El-Tahe,., ER Shaaban., EE Massoud., ME Mahmoud., Enhancement and optimization of gamma radiation shielding by doped nano HgO into nanoscale bentonite. Nuclear Engineering and Technology 54, 6, PP. 2253-2261. 2022.

[13] U Rilwan, MA Abdulazeez, I Maina, OW Olasoji, Atef El-Taher, Islam G Alhindawy, KA Mahmoud, MI Sayyed, Mohamed Elsafi, M Rashad, Yasser Maghrbi. ., 2025 The use of coconut shell ash as partial replacement of cement to improve the thermal properties of concrete and waste management sustainability in Nigeria and Africa, for radiation shielding application. Scientific African 27, 02578

[14] HH Negm, EA Allam, E Abdeltwab, M Mostafa, ME Mahmoud, A. El-Taher., 2024 A new nanocomposite of copper oxide and magnetite intercalated into Attapulgite clay to enhance the radiation shielding. Radiation Physics and Chemistry 216, 111398

[15] R M El-Sharkawy, M Almeshari, Y Alzamil, A Abanomy, B Alshoumr, A M Halbas, E A Allam, M E Mahmoud, HA Saudi, AEl-Taher., Doping of steel slag waste as a sustainable filler in ceramic tile composites for enhanced gamma-ray shielding. Materials Advances 6 (18), 6305-6319. 2025.

[16]. A. S. Ouda, Development of high-performance heavy-density concrete using different aggregates for gamma-ray shielding. *Progress in Nuclear Energy*, *79*(1), 48–55, 2015.

[17]. W. D. Callister, & D. G. Rethwish, Materials Science and Engineering: An Introduction (10^{th} Ed.).

[18]. M Almeshari, F Sallam, M Tharwat, Y Alzamil, M Salih, B Alshoumr, A Alyahyawi, A El-Taher., Preparation and structure investigation of polyethylene terephthalate polyester reinforced Ni0. 5Zn0. 5Fe2O4 nanoparticles for gamma ray shielding performance. Physica Scripta 99 (5), 055311. 2024.

[19] Rehab M El-Sharkawy, Meshari Almeshari, Yasser Alzamil, Ahmad Abanomy, Bader Alshoumr, Asmaa M Halbas, Elhassan A Allam, Mohamed E Mahmoud, HA Saudi, Atef El-Taher., 2025 Doping of steel slag waste as a sustainable filler in ceramic tile composites for enhanced gamma-ray shielding. Materials Advances 6 (18), 6305-6319